The MAGIC gamma-ray telescope: status and first results

Enrique Fernandez[a]

[a]Institut de Física d'Altes Energies/Univ. A. de Barcelona,
Campus UAB, Edif. Cn
08193 Bellaterra, Barcelona, Spain
e-mail: enrique.fernandez@ifae.es

MAGIC, a 17 m diameter Cherenkov telescope for gamma ray astronomy, has recently been commissioned at the Roque de los Muchachos site in the Island of La Palma, of the Canary Islands. The telescope was proposed in 1998 with the goal of lowering the threshold of observation of gamma rays by ground detectors to 20-30 GeV energies. This paper describes its main design features, its physics objectives and its first operations.

1. The MAGIC telescope

MAGIC, [1] (Major Gamma-ray Imaging Cherenkov telescope) is a gamma-ray telescope which images the Cherenkov light created by the showers of high energy gamma rays in their collisions with the upper atmosphere. The telescope is located in the *Roque de los Muchachos Observatory* (ORM) of the island of La Palma, in the Spanish Canary Islands, at 28.8 N, 17.9 W and 2200 m altitude. The ORM is also the site of several European optical observatories due to the excellent observational conditions and infrastructure.

The telescope was formally inaugurated in October of 2003. Commissioning [2],[3] started shortly afterwards and has continued throughout 2004, interspersed with several "physics runs", during which several sources were observed. First results have been shown in March of 2004 [4]

The telescope operates with the imaging Cherenkov technique pioneered by the Whipple collaboration [5]. The atmosphere acts as a calorimeter for the incoming high energy gamma-rays. These collide with the molecules of the upper atmosphere initiating electromagnetic showers. The electrons and positrons from the shower are ultra relativistic and emit Chrenkov light. The angular aperture of the light is determined by the Cherenkov angle which varies with altitude from 0.4 at 20 km to 1.3 degrees at ground level. The light from the shower illuminates a circular area at ground level quite uniformly up to a radius of about 130m, and rapidly decreasing for larger radii. The radius is quite independent of the primary gamma-ray energy, since it depends primarily on the Cherenkov emission angle. The Cherenkov light arrives almost instantaneously, in 2-3 ns, as it is easy to understand from the fact that the secondary electrons and positrons of the shower travel at speeds very near that of light. The spectrum of this light extends from 300 to 600 nm but a significant fraction of photons are absorbed due to Rayleight and Mie scattering. The resulting spectrum at ground level peaks at 330nm in the near ultraviolet. The telescope consists on a reflector that focuses the light into a camera made of an array of fast photomultiplier tubes. The telescopes operated in this way are known as Imaging Atmospheric Cherenkov Telescopes (IACT's).

The total amount of light is proportional to the total path of the secondary electrons and positrons of the shower, which is in turn proportional to the energy of the primary particle. With a telescope located anywhere inside the light pool one is able in principle to detect the shower, and, assuming uniform illumination, infer the energy of the primary gamma. The intensity of the light (number of photons per unit area) is very small, about 5 photons per m^2 for a vertically incident 100 GeV gamma. But the fact that it arrives during a very short time makes its detection possible above the background (see below). Furthermore the reflector creates an image of the shower at the focal plane which can be resolved with a segmented camera, each pixel in the latter corresponding to a PMT. The light arrives as a disk, but the optics of the reflector is such that the image appears in general as an ellipse whose elongation and orientation depend on the alignment of the telescope with the axis of the shower and on where the telescope is located with respect to the light disk (the impact parameter).

The main background is of two kinds. First there is the background caused by the light of the night sky (NSB for short) produced by starts, Moon reflections, de-excitation of atmospheric molecules and other sources. This background is constant or varies slowly during the night and is rejected by the trigger requirements, which demand a coincidence in time of several neighboring pixels. The other type of background is that caused by incoming charged cosmic rays which generate hadronic showers. These are much more frequent than gamma rays but a high rejection power is achieved by the analysis of the image. First of all electromagnetic showers are compact and their image appears as a regular ellipse on the camera plane. By contrast hadronic showers are more scattered and produce images which deviate from the regular ellipse shape. A second characteristic is that the expected gamma signals come from a source at a fixed direction while charged cosmic rays come from all directions. This feature can be exploited if the telescope is pointing towards the source, whose position is known a priori. If this is the case, the major axis of the ellipse for gammas coming from the source points towards the center of the image plane, while that from cosmic rays coming from other directions does not. Figure 1 illustrates these features. Also in the figure is the image of a muon track moving along the axis of the telescope. Muons can also be a source of background as well as primary electrons, and this can become important at the minimum energy at which MAGIC will be able to operate, see for example [7].

The detailed analysis of the images is done in terms of the so-called Hillas parameters [6]. In particular the parameter α is the angle of the major axis of the shower with respect to the straight line defined by the center of the shower and the center of the image plane. A signal of a source appears as a peak at zero α over the background produced by charged cosmic rays. See below in the data taken with MAGIC.

This technique should be contrasted with that of the extended shower arrays [8], with which one tries to observe directly the tail of the shower, at ground level, typically with an array of detectors placed in a matrix over an extended area. With this method one is able to detect only very high energy primary particles, capable of producing a shower with enough secondaries reaching the ground. Recall that the atmosphere has a thickness of about 28 radiation lengths at see level. The imaging technique is also different from the air-fluorescent detectors, which directly observe the shower from the fluorescent light of excited Nitrogen molecules. But the light yield for air-fluorescent is very small and this technique is only suitable for energies above 10^{17} eV. Up to now, all the sources emitting at very high energies (see below) have been discovered with IACT's.

2. MAGIC design goals

The main MAGIC design goal was to be able to observe gamma rays with as low as possible energy. The main motivation for such a requirement is illustrated in Figure 2. While at low energies (up to 10 GeV) many gamma-ray sources have been established, there are only a handful of sources known to emit at energies above 300 GeV. Up to very recently the situation was as in Figure 2 (bottom). Although most sources exhibit a decreasing power law spectrum, the extrapolation of figure 2 (top) to higher energies implies that many sources should be observable in the region between 10 GeV and 300 GeV. This region of the electromagnetic spectrum remains mainly unexplored. Experiments in satellites have too

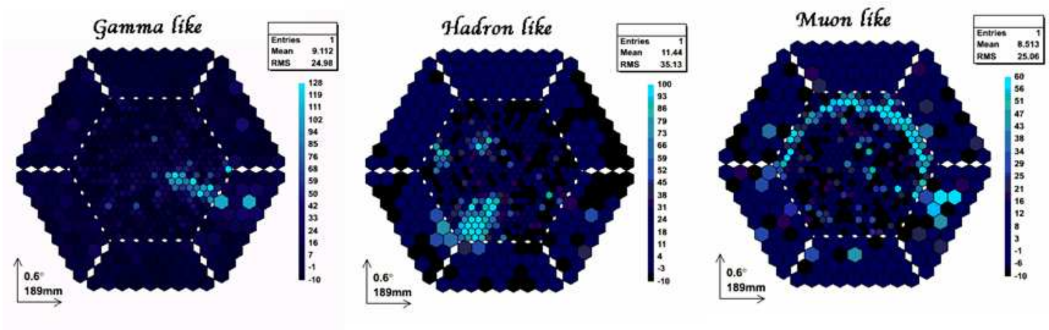

Figure 1. The left-most figure is the image of a gamma-ray taken with MAGIC. One can see the ellipse form of a shower, pointing to the center of the camera plane. At the center there is the image of a hadronic shower, which is more scattered than that of a gamma. The image on the right is of a muon moving in a direction very closed to that of the telescope axis.

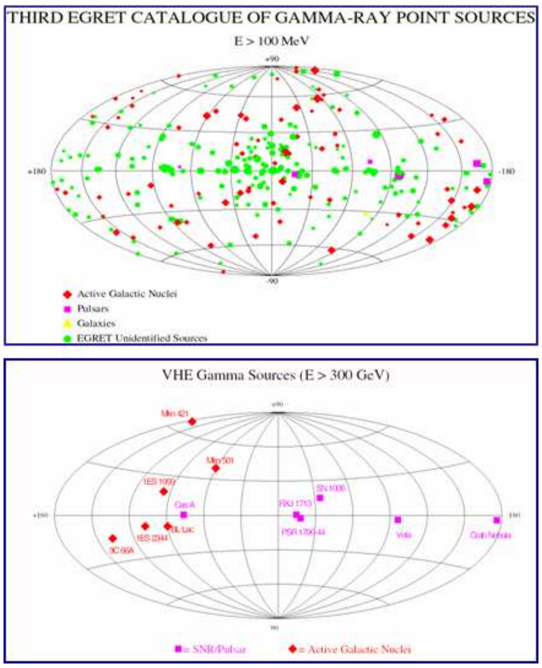

Figure 2. The upper figure is the catalog of sources of gamma-rays observed by the EGRET experiment on board of the Compton Gamma-Ray Observatory, extending up to about 10 GeV. The lower figure is the list of sources above 300 GeV seen from ground-based instruments, up to the year 2003.

low an area to be able to observe sources above 10 GeV, since the already mentioned sharply decreasing power law energy spectrum implies too low counting rates in the detectors employed up to now. On the other hand experiments on the ground, including Cherenkov telescopes, have only been able to observe very high energy gammas, above 300 GeV.

To understand the threshold energy of Cherenkov telescopes one has to realize that the Cherenkov photons from showers have to be detected on top of the NSB mentioned in the previous section. The fluctuations on this constant background will scale with the square root of the reflector area while the number of signal photons, which is proportional to the energy, will increase with the area. Therefore, roughly speaking and other parameters aside, the signal over background, and thus the sensitivity of the detector, should increase as the square root of the area. In MAGIC it was decided to build as large as possible telescope as it was considered feasible at the time, a 17m diameter reflector, with an area of 234 m^2 (Figure 3).

Another design feature was dictated be the goal of observing the follow up of gamma-ray bursts. Although the average duration of gamma-ray burst is of the order of one minute there are

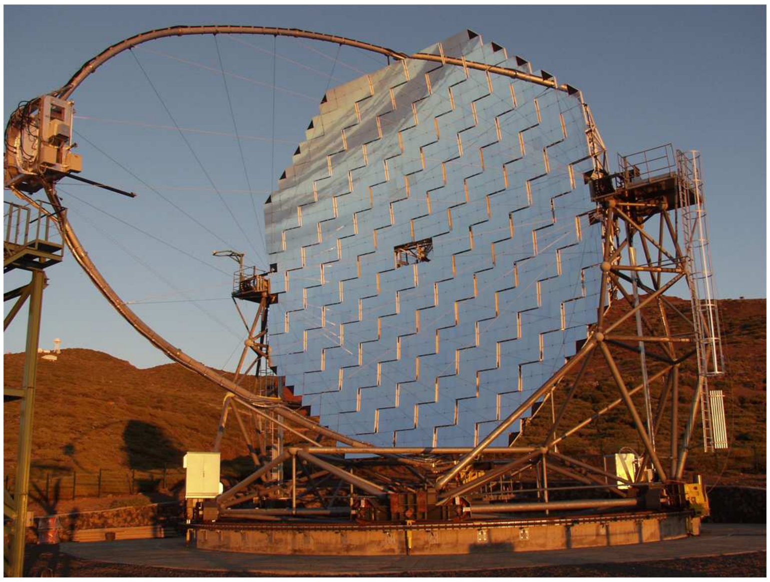

Figure 3. A recent photograph of the MAGIC Telescope.

cases when the burst lasts much longer. A network of detectors world-wide alerts of their presence and transmits their location. MAGIC was designed to move to any position in the sky in less than half a minute. In the future the intention is to prepare the telescope to respond to the alarm and automatically point it to the GRB, and thus explore is there is high energy gamma radiation associated to it. Because of this requirement the structure of the telescope had to be kept very light, made with rods of carbon fiber reinforced with aluminum at the ends (Figure 4). The weight of the entire telescope is approximately 65 tons and that of the dish and mirrors 20 tons. The fast slewing has been achieved: the telescope has been moved 180 degrees in azimuth in 22 seconds, with the motors at full power.

3. Some other design features

The main elements of the telescope are the following

1. An alt-azimuth mount The telescope can be rotated to any position in azimuth by means of two powerful motors. Another

Figure 4. A detailed view of the structure of the MAGIC frame, showing the tube-knot system. The light frame is important for a fast slewing of the telescope.

motor controls the declination from -80^0 to $+105^0$. As already mentioned the design goal is to move to any position within the allowed range in less than half a minute.

2. A parabolic reflector. The reflector consists of a tessellated mirror with a total area of 234 m^2. The individual mirrors have an area of 50x50 cm^2. There are 956 mirrors, each consisting of a 5 mm thick plate made of an AlMgSi1.0 alloy, glued to honeycomb structure sandwich made of aluminum. The plate is diamond milled in an spherical way with an appropriate radius depending on its position in the overall parabolic reflector. The plate is protected from aging by a thin quartz layer. The mirrors are grouped into panels of 3 or 4, and each panel can be oriented independently by a control system to correct for possible deformations of the structure when repositioning the telescope. The focal distance of the telescope is equal to the diameter. The point spread function after alignment is 0.04^0.

3. A finely pixelated camera using advanced hemispherical PMT's. The camera consists of an array of 576 PMT's covering a circular area of 1.5 m diameter. It has a 4^0 field of view (FOV) and it is divided into two sections. The inner hexagonal section is equipped with 397 0.1^0 FOV PMT's (1 inch diameter). It is surrounded by an outer section with coarser pixels consisting of PMT's of 0.2^0 FOV (1.5 inch diameter). The use of coarser pixels reduces the cost without degrading the quality of the image, which is already limited in this area by coma aberrations. The PMT's are from the company Electron Tubes and have 6 dynodes for low-gain. Operation at low-gain is important to prevent damage from the NSB or during moonshine. Each PM has a light catcher in front, which combined with a hemispherical photo-cathode gives a high probability that the photons traverse the photocathode twice, thus increasing the conversion probability (Figure 5). The average quantum efficiency in the range 300-600 nm was measured to be 20% [9]. It was later discovered that coating the PM outer surfaces with a Wavelength Shifter increased the QE up to 30% and extending it to the UV range [10]. The camera, which weights 450 kg, is supported by a single aluminum arch, secured against transverse displacements by prestressed steel cables [3] (see Figure 3).

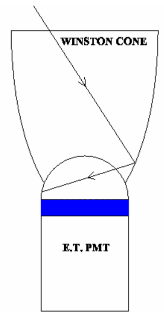

Figure 5. Schematic of the light collection in the photomultiplier tubes.

4. Signal amplification and transmission system. The fast signals from the PMT's are amplified by an ultra-fast trans-impedance amplifier, already in the camera housing. The amplified signals are transmitted analogically over 162 m long optical fibers using VCSELs (Vertical Cavity Surface Emitting Laser Drivers). After transmission the signal is split with one branch going to the trigger system and the other being digitized (after some processing) by 8-bit 300 MHz FADCs.

5. Trigger and DAQ systems. The trigger is a two-level system with programmable logic [11]. The first level uses 19 hexagonal overlapping cells of 36 pixels each, covering 325 of the inner pixels. It applies time coincidences and next neighbor logic. The second level can be used to perform rough analysis

and apply topological constraints on the event images.

The digitized samples are put in ring buffers to wait for the trigger decision. The dead time is less than 0.1% at the design trigger rate of 1kHz. The data rate at the output is 20 MB/s which produces up to 800 GB raw data per night.

4. MAGIC physics program

Figure 6 illustrates some of the physics goals of MAGIC. They cover the astrophysics of sources as well as measurements of interest in cosmology, such as the search for dark matter of the measurement of the event horizon for putative distance sources. However it should be emphasized that this field is really new and many of the physics topics that will be studied will presumably be driven by the observations themselves. See references [12], [13] for general reviews of gamma-ray astronomy. The number of known sources above

Figure 6. Illustration of some of the physics topics that can be studied with MAGIC.

300 GeV is really very “small” as shown in Figure 7 which list the known TeV sources (up to 2003) [14]. Among the galactic sources three are Plerion Pulsars. These are rapidly rotating neutron stars, left over from Supernova explosions. The radiation from the supernova remnant fills a complete area around the pulsar and hence the name ”plerion”. Other three sources are Shell Supernova Remnants, and the other sources, except for the galactic center, are not yet well established. The extragalactic sources are mostly Active Galactic Nuclei of the BL-LAC type.

Some of the studies planned for MAGIC are the following:

Study of Plerion Pulsars.

The prototype Plerion Pulsar is the Crab Nebulae, which is the standard candle of gamma-ray astronomy. The emission from the Crab Nebulae has two components: a pulsed component with a 33ms period (spinning down with at a rate of $422 \times 10^{-15} s/s$, extending to 10 GeV or higher, and a steady component which goes from 10 MeV to very high energies, above 300 GeV, the later being that observed by gamma-ray telescopes. Much has been learned from studying this source at wavelengths going from radio to TeV energies [15].

The pulsed emission originates close to the pulsar, coming from synchrotron radiation of VHE electrons inside the so called light cylinder, whose surface is the region of the pulsar where the velocity of the rotating matter reaches that of light. Two models have been proposed for the origin of the radiation, which differ in the region where it originates: in the Outer-Gap model the radiation originates in the pulsar magnetosphere while in the Polar-Cap model the radiation originates near the magnetic poles [16]. The two models predict a somewhat different extinction of the pulsed emission at energies between 10 and 50 GeV, a region which MAGIC can explore.

The non-pulsed TeV emission is thought to

Table 1
Source Catalog c.2003

TeV Catalog Name	Source	Type	Discovery Date/Group	EGRET 3rd. Cat.	Grade
TeV 0047−2518	NGC 253	Starburst	2003/CANG.	no	B*
TeV 0219+4248	3C66A	Blazar	1998/Crimea	yes	C−
TeV 0535+2200	Crab Nebula	SNR	1989/Whipple	yes	A
TeV 0834−4500	Vela	SNR	1997/CANG.	no	C*
TeV 1121−6037	Cen X-3	Binary	1999/Durham	yes	C
TeV 1104+3813	Mrk 421	Blazar	1992/Whipple	yes	A
TeV 1231+1224	M87	Radio Gal.	2003/HEGRA	no	C
TeV 1429+4240	H1426+428	Blazar	2002/Whipple	no	A*
TeV 1503−4157	SN1006	SNR	1997/CANG.	no	B*
TeV 1654+3946	Mrk 501	Blazar	1995/Whipple	no	A
TeV 1710−4429	PSR 1706−44	SNR	1995/CANG.	no	A
TeV 1712−3932	RXJ1713.7−39	SNR	1999/CANG.	no	B+*
TeV 2000+6509	1ES1959+650	Blazar	1999/TA	no	A*
TeV 2032+4131	CygOB2	OB assoc.	2002/HEGRA	yes†	B
TeV 2159−3014	PKS2155−304	Blazar	1999/Durham	yes	A*
TeV 2203+4217	BL Lacertae	Blazar	2001/Crimea	yes	C*
TeV 2323+5849	Cas A	SNR	1999/HEGRA	no	B*
TeV 2347+5142	1ES2344+514	Blazar	1997/Whipple	no	A*

† CygOB2 lies within the 95% error ellipse of the EGRET source 3EG J0233+4118.

Figure 7. The galactic and extra-galactic high energy gamma ray sources known in 2003, taken from [14].

originate in the supernova remnant through inverse Compton scattering of the electrons on their own radiation (synchrotron self-Compton model, SSC). A cutoff of the soft component (the target photons) has been seen in the data. The transition from pulsed to non-pulsed emission is also of interest and this may occur in the region that MAGIC can explore.

Shell Supernova Remnants.

Shell Supernova Remnants (SR) are the other type of galactic sources emitting at very high energies. They have been considered as potential sources of galactic cosmic rays. The acceleration would take place in the expanding shock (first order Fermi acceleration), that is, towards the rings of the nebula. However all the 3 known TeV gamma sources are weak. Furthermore many of the EGRET sources should emit at TeV energies if the gammas are produced by protons interacting with molecular clouds but they do not. These facts point to an electron origin of gamma radiation (again by inverse Compton scattering of the electrons on ambient photons) and not to proton acceleration, required if they were sources of cosmic rays. The goals of MAGIC will be to study the end point of the very high energy emission and to pinpoint from where in the shell the gammas originate.

Active Galactic Nuclei.

About five percent of the galaxies are "active", in that they emit non-thermal radiation. A "universal model" [13] to explain the many different types of existing objects is depicted in Figure 8. At the center of the galaxy there is a very massive black hole of between 10^6 to 10^9 solar masses. The hole is accreting mass which forms a thin disc rotating at relativistic velocities and a torus several light years thick. The disc emits thermal radiation up to KeV energies. Matter not only falls into the black hole, but it is also ejected in two opposite jets, at relativistic speeds, with Lorentz factors as high as 10. The scale of this jets can be enormous, up to 10^6 light years.

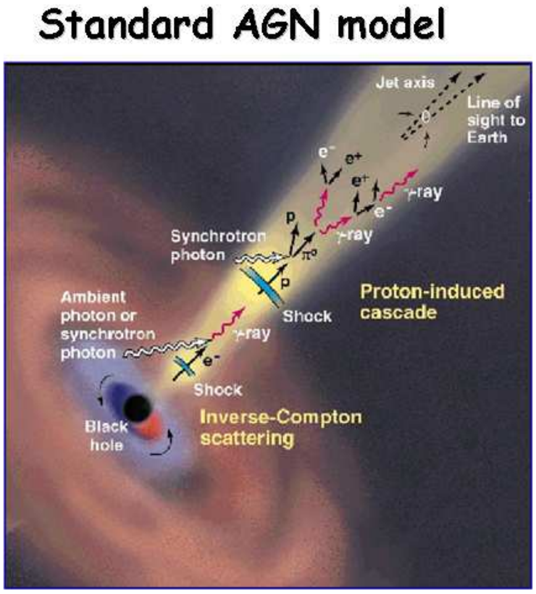

Figure 8. Scheme of an active galactic nucleous.

Different types of AGN's (Seyfert 1 and 2, radio loud, radio quiet, broad band, narrow band) result depending mainly of the relative orientation of the jets with respect to the line of sight (and to a lesser extent on other parameters, such as the distribution of matter in the disk and torus). The luminosity of the AGN increases drastically when the jet points to the observer producing a Blazar. More than 50 Blazars have been observed by the EGRET detector, emitting up to GeV energies. A few Blazars also emit at TeV energies, such as Mkn-421 and Mkn-501, all of then are BL-Lac objects, named from the first seen, in Lacerta.

Figure 8 also illustrated the different types of radiation that can emanate from the jet. Shock acceleration can accelerate both electrons and protons. The electrons emit synchrotron radiation and, through inverse Compton scattering, effectively accelerate gammas, either those emitted by synchrotron radiation (the Synchrotron Self Compton Model already mentioned) or other ambient photons, at high energy. Shock accelerated of protons would also produce high energy gammas. The protons could collide with photons resulting in photoproduction of high energy pions of which the neutral component would produce high energy gammas.

Previous observations have seen a correlation between the x-rays and the VHE emission, although there are also cases where this correlation has not been seen. Most of these sources show strong time variability over long periods, and also over shorter periods [17], [18], as short as 15 minutes, indicating that the emitting region is very small. A time correlation between the gamma-ray and x-ray emission has also been reported, which points towards an electromagnetic origin of gamma ray emission.

The study of the time variability would be greatly enhanced with a sensitive telescope such as MAGIC. The period of variability gives an upper limit for the size of the system. It has also been used to put a limit on the scale of quantum gravity.

Study of Event Horizon.

The low energy threshold of MAGIC would allow the observation of sources at cosmological distances, which is not possible for higher energies. The reason is that high energy gammas interact with the extragalactic background light (EBL) and are absorbed. The dominant process is

$$\gamma_{high-energy} - \gamma_{target} \rightarrow e^+e^-$$

which has a peak at $E_{cm} = 1.8 \times (2m_ec^2)$. There is some evidence for this cut-off in the data seen by the HEGRA collaboration [19].

The extragalactic background light is not very well known, particularly in the infrared part of the spectrum. But even allowing for uncertainties on the EBL it is safe to assert that below 30 GeV the universe becomes quite transparent to gamma rays (Fig. 9) [21]. A telescope being able to

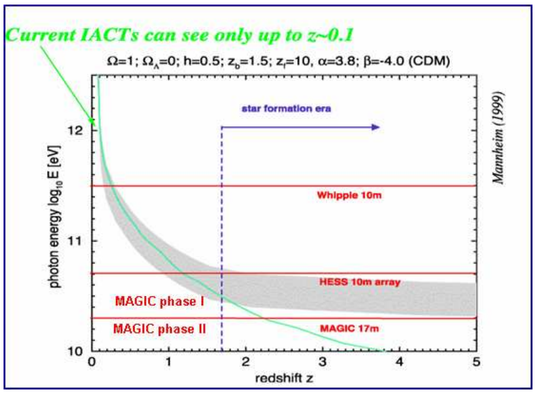

Figure 9. The gamma ray horizon for different threshold energies taken from [21].

detect gammas at these energies should be able to see very far, at cosmological distances reaching to $z = 1.5$ or beyond. If a sufficiently large sample of AGN's at different redshifts is observed, the data can be used to constraint the extra galactic background light.

Inversely, if an energy cut-off, attributed to the absorption of the gamma rays by the EBL, is seen in a distant source, its distance can be computed by integration of the collision probability of the gamma with the EBL along the path from the source to the observer. If the red-shift of the source is known independently, one then has a relation between distance and red-shift, a relation which depends on the cosmological parameters.

The idea is then to measure the gamma-ray-horizon (and thus the distance, assuming a known EBL) to several sources at different red shifts. To establish that the cut-off in the energy is due to the absorption by the EBL and not to an extinction at the source itself, one would need to measure several AGN's at similar red-shifts, and see that all show a cut-off at similar energies. Shown

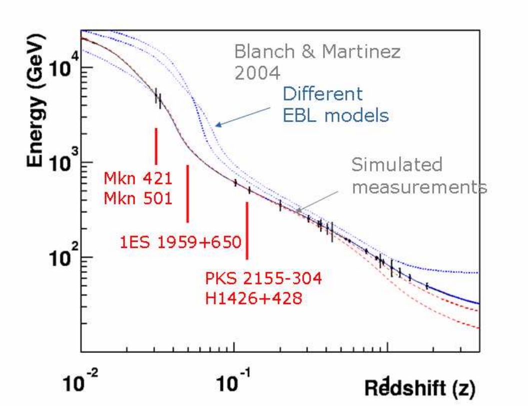

Figure 10. The gamma-ray horizon versus redshift for a number of simulated sources, from [22].

in Fig. 10 is a simulation of the gamma-ray-horizon versus red-shift for a number of sources, at distances accessible by MAGIC [22]. The curves are for different cosmological parameters. In Fig. 11 one can see the projections in the Ω_Λ versus Ω_M. The different contours are for different assumptions on the EBL. This measurement of the correlation is independent from other measurements such as those provided by type 1a Supernovae, anisotropies of the microwave

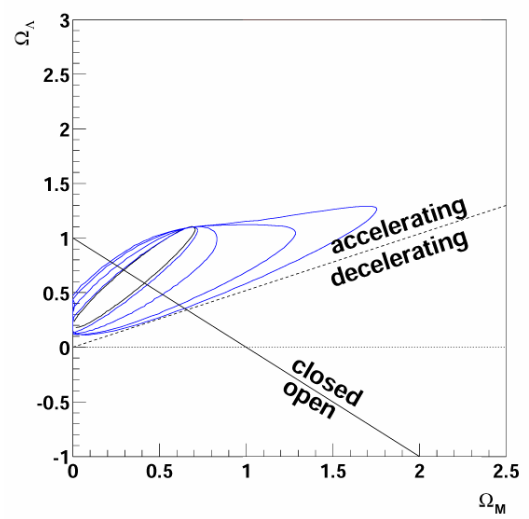

Figure 11. The contour regions for $\Omega_\Lambda - \Omega_M$, from a simulated number of observations of AGN's, from [22].

background radiation and large-scale structure.

5. Status of MAGIC

As mentioned above the telescope was inaugurated in October of 2003. During the present year several sources have been observed. The results are yet very preliminary. Just as an example Figure 12 shows the data on the Crab nebula analyzed with tight cuts, in particular the parameter *size* (number of estimated photons converting in the camera) was required to be above 2000 corresponding to an energy in excess of 100 GeV. A clear peak is seen in the α parameter at $\alpha = 0$ as expected. Another example is Figure 13 in which the Markarian 421 (an AGN at $z = 0.03$) was analyzed for three intervals of the parameter *size*. The lower interval corresponds to energies of about 80 GeV. The significance of the observation increases with size.

It should be remarked that the analysis at low energies (meaning here below 100 GeV) becomes more difficult and the conventional Hillas param-

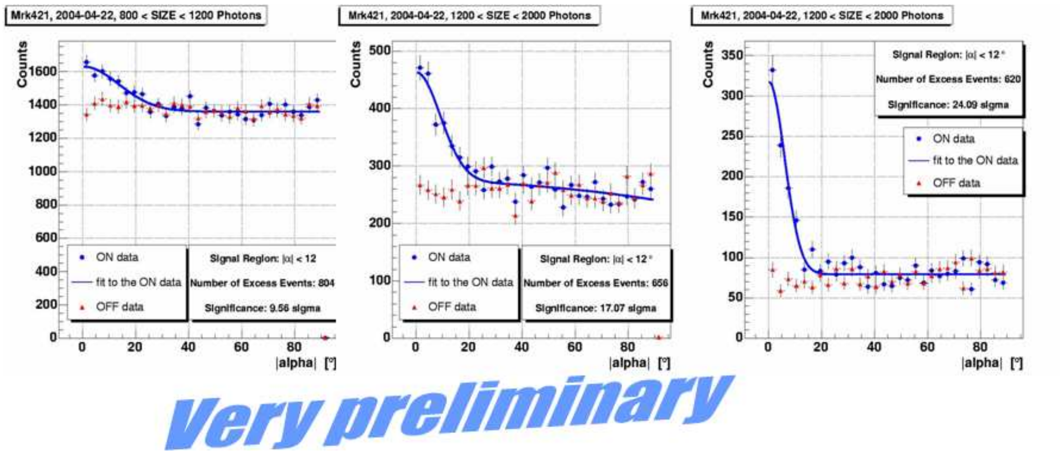

Figure 13. Data on Markarian 421 taken with MAGIC. The 3 plots correspond to different energy intervals.

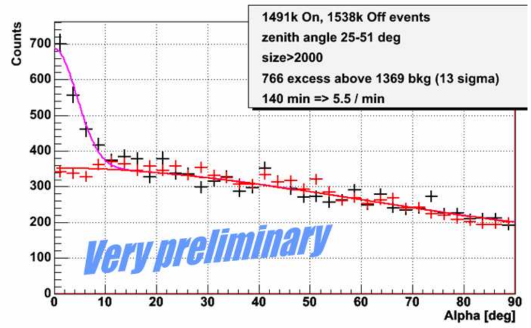

Figure 12. Data from the Crab nebulae taken with MAGIC.

eters are not fully adequate for extracting the signal and separating it from the background. At the lower end of the observational window, around 20 GeV, the light pool from the shower arriving at the ground is no longer uniform. The geomagnetic field has also an effect on the trajectories of the secondary electrons and positrons in the shower, which should be taken into account. New methods and calibrations are being actively pursued to be able to analyze the events at these energies.

6. Conclusion

The MAGIC Telescope is now fully operational in its final configuration. After the usual start-up problems several successful observations of sources have already taken place and the telescope is now being calibrated. The development of new methods for observing at low energies is in progress.

7. Acknowledgements

I thank the organizers, Leo Resvanis, Stratos Anassontzis and Spyros Tzamarias for the invitation to give the talk and for the excellent organization of the workshop in such a beautiful place as

Pylos, and Kostas Papageorgiou for all the help during the conference and for the very pleasant company in visiting the site. I also thank Manel Martínez for the discussions on the physics of high energy gamma rays and for a careful reading of this paper. And to the whole MAGIC collaboration for making MAGIC real. This work is supported by grant FPA2003-00417 of the Spanish Ministry of Science and Education.

REFERENCES

1. J. A. Barrio et al., The MAGIC Telescope Design report, MPI Report MPI-PhE/98-5 (March, 1998). MAGIC is a collaboration between the following institutions: IFAE Barcelona, Univ. Autònoma Barcelona, Crimean Observatory, Univ. California at Davis, Univ. of Lodz, Univ. Complutense Madrid, INR Moscow, MPI München, INFN/Univ. Padua, INFN/Univ. Siena, Univ. Berlin, Tuorla Observatory, Yerevan Phys. Institute, INFN/Univ. Udine, Univ. of Würzburg and ETH Zrich.
2. C. Baixeras et al., Commissioning and first tests of the MAGIC Telescope, NIM A518 (2004) 188.
3. Eckart Lorenz, Status of the 17m diameter MAGIC Telescope, New Astrn. Rev. 48 (2004) 339.
4. Schweizer, T. et al., Status report of the MAGIC Telescope, Contribution to DPG (German Physical Society) Spring Meeting, Mainz, March 2004.
5. See for example T. C. Weekes, Phys. Rep. 160 (1988) 1, and references therein.
6. A. Hillas, Proc. 19th ICRC La Jolla (1985).
7. J. Albert et al., Building a low-energy threshold gamma-ray telescope, submitted to Astroparticle Physics.
8. For a review of the gamma detection techniques see for example J. W. Cronin, K. G. Gibbs and T. C. Weekes, Annu. Rev. Nucl. Part. Sci., 43 (1993) 883.
9. A. Ostankov et al., NIM A442 (2000) 117.
10. D. Paneque et al., A Method to Enhance the Sensitivity of Photomultipliers for Air Cherenkov Telescopes. Submitted to NIM.
11. D. Bastieri et al., A two-level pattern trigger for the MAGIC telescope, NIM A461 (2001) 521.
12. R. A. Ong, Phys. Reports, 305 (1998) 94.
13. C. M. Hoffman, C. Sinnis, P. Fleury and M. Punch, Gamma-Ray Astronomy at High Energies, Rev. Mod. Phys., 71(4) (1999) 897.
14. D. Horan and T. C. Weekes, New Astron. Rev. 48 (2004) 527 (astro-ph/0310391).
15. O. C. de Jager, Proceedings of XXVII International Meeting on Fundamental Physics, Acta Physica Polonica B30 (7) (1999) 2293.
16. J.K. Daugherty and A. K. Harding, ApJ 458 (1996) 278.
17. J. A. Gaidos et al., Nature 383 (1996) 319.
18. A. Aharonian et al., A&A, 342 (1999) 69.
19. A. Aharonian et al., A&A, 349 (1999) 11.
20. Krawczynski et al., ApJ 601 (2004) 151.
21. K. Mannheim, Rev. Mod. Astron. 12 (1999) 101.
22. O. Blanch and M. Martinez, astro-ph/0107582 and astro-ph/0406061.